Journal of Theoretical and Applied Physics, **4**-3, 1-7 (2010)

Structure-controlled synthesis of single-walled carbon nanotubes with non-magnetic-catalyzed plasma CVD and their electronic Properties

Z. Ghorannevis[1,2,*], T. Kato[2], T. Kaneko[2], R. Hatakeyama[2]

[1]*Plasma Physics Research Center, Science and Research Branch, Islamic Azad University, Tehran, Iran*
[2]*Department of Electronic Engineering, Tohoku University, Sendai, Japan*

Received: 1 April 2010/Accepted: 8 March 2010/ Published: 20 December 2010

Abstract

This work covers the analysis of the nonmagnetic-catalyzed plasma chemical vapor deposition (PCVD) of single-walled carbon nanotubes (SWNTs). The selective growth of SWNTs by the nonmagnetic catalyst using PCVD is realized for the first time. Experimental investigations are presented, which allow to get a comprehensive picture of the nonmagnetic catalytic growth of SWNTs by PCVD. The PCVD growth of SWNTs is performed on an alumina supported Au catalyst using methane as a carbon source. The methodologies to accomplish the controlled growth of SWNTs, i.e., diameter, density, and chirality are investigated. The Au catalyst can afford the SWNTs growth with narrow diameter and chirality distribution with PCVD by carefully adjusting the experimental parameters. Methane PCVD on the Au catalyst under well defined conditions produced predominantly (6,5) SWNTs according to Raman, UV-Vis-NIR absorption, and photoluminescence excitation/emission (PLE) spectroscopic characterizations. The high yield of (6,5) semiconducting SWNTs produced by the structure controlled synthesis described above is promoted us to directly use the as-synthesized SWNTs for constructing nanotube field effect transistors (FETs), which suggests the SWNTs grown from the nonmagnetic catalyst with PCVD display the best device performance in comparison with thermal chemical vapor deposition (TCVD) synthesized and magnetic catalyzed SWNTs based devices. Based on the magnetic measurements with the Au catalyzed SWNTs, we observe that the nonmagnetic catalyzed SWNTs show ferromagnetic features, which suggest that the ferromagnetic features might come from the SWNTs itself. Hence this narrow-chirality distributed Au catalyzed SWNTs selectively grown with PCVD could be attractive to both fundamental studies of intrinsic magnetic properties of SWNTs and industrial applications to nanoelectronics.

***PACs*:** 61.48.De; 81.07.De; 61.46.Np; 81.15.Gh
Keywords: *Single-walled; Carbon nanotubes; CVD; Plasma; SEM; TEM*

1. Introduction

The unique properties of single-walled carbon nanotubes (SWNTs) [1,2] have motivated intense researches in the fabrication of electronic components [3], field emission sources [4], and hydrogen storage devices [5]. Certain carbon nanotube (CNT) applications require specific dimensions and different levels of homogeneity (e.g. diameter, length, reactivity, crystallinity, purity, and chirality) [6]. Since the composition and morphology of catalyst nanoparticles are critical in determining the structure, length, and yield of nanotubes, differences of methods and catalysts include superior possibility for the detailed structure control of CNTs. The structures of SWNTs such as diameter and chirality are known to depend on the kinds of catalysts and growth methods [7-10]. During this last decade, it was a common sense that only transition-metal catalysts such as Fe, Co, and Ni mainly play dominant catalytic roles in the growth of SWNTs. Recently many other catalysts such as, Au, Ag, Cu, Pd [11], Rh [12], Mg, Mn, Cr, Al, Sn [13] and also semiconductor particles such as Si and Ge [14] have been reported to be useful for the SWNT growth by TCVD. This finding of these novel-type catalysts expanded the possibility of the further precise control of SWNT structures by adjusting the catalyst type and the growth method. Up to now, these novel-type catalysts have been utilized only in TCVD and there is not any report for the growth of SWNTs from such novel-type catalysts by PCVD [15,16] which is known to be able to realize a freestanding [17], low temperature [18], and semiconductor rich [8,19] growth of high quality SWNTs. Base on this background, we attempt to grow SWNTs by PCVD from nonmagnetic Au, Pt, and Ag catalysts, which are one of the novel-type catalysts. The elucidation of different SWNT growth kinetics between the previously well-known magnetic catalysts and such novel-type nonmagnetic catalysts was also addressed.

2. Experimental

SWNTs synthesis contains two steps. First step is catalyst preparation, where catalytic thin films of X

*Corresponding author: Zohreh Ghorannevis;
E-mail: z.ghorannevis@gmail.com
Tel: (+98) 21 44869627
Fax: (+98) 21 44869626

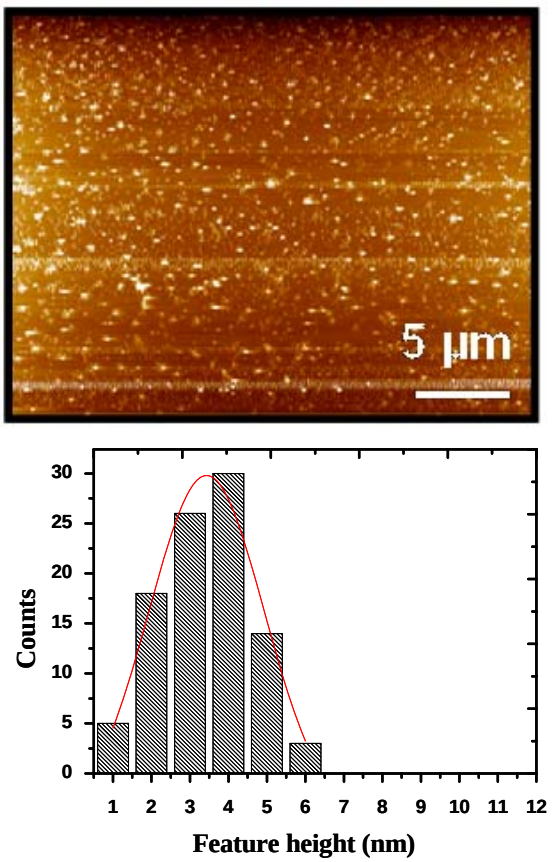

Fig. 1. AFM image and size distribution of Au nanoparticles

(~ 0.2 nm) / Al_2O_x (20 nm) are sequentially prepared on substrates by a vacuum evaporation and a sputtering, where X denotes Au, and Fe. Fig. 1 is the atomic force microscopy (AFM) image and corresponding size distribution of the Au nanoparticles estimated from the height profile image. The SWNTs growth was carried out by PCVD [14] and TCVD with methane-hydrogen mixture gasses (Fig. 2). In case of PCVD, Methane-hydrogen decomposition was performed using a radio-frequency (RF; 13.56 MHz) plasma reactor. The RF power (P_{RF}) was supplied to an upper electrode and a mesh grid was used as an anode to promote spatial diffusion of plasmas. A substrate was placed on a heater which is located underneath of the lower electrode. The distance between the lower electrode and the substrate was fixed at 50 mm. The growth of SWNTs by PCVD was carried out with following procedures. First, the system was pumped down to a base pressure of 1 Pa with a rotary pump, and the substrate was heated up to 700 ~ 720 ^oC.

Methane and hydrogen gasses were then introduced for the SWNT growth. When the total pressure reached 50 Pa, the P_{RF} of 50 W was applied to produce plasmas and the SWNT growth was started. The growth time was 1 min. After the SWNT growth, the methane and hydrogen gases were pumped out and Ar gas was introduced into the system in order to cool down the substrate. The same setup was used for TCVD synthesis while P_{RF} was off. The differences in the TCVD synthesis process without PCVD case were pretreatment of the Au catalyst, growth temperature, and growth time. It was found that in case of TCVD, the Au catalyst preheating in air is necessary. And SWNTs could not be grown without preheating in air. Also the growth time and growth temperature were 15 min, and 750 ~ 800 ^oC, respectively.

3. Results and Discussion

Figures 3 (a-c) and (d-f) show the Raman spectra of the Au SWNTs synthesized with PCVD and TCVD, respectively. As it can be seen the growth temperature and growth time in case of PCVD is lower and shorter then that for TCVD, respectively. Also PCVD growth of SWNTs using the nonmagnetic catalyst, which has the lower catalytic activity for SWNTs growth can be performed even without any catalyst pretreatments. The highly decomposed source gas in PCVD can play a significant role in a surface

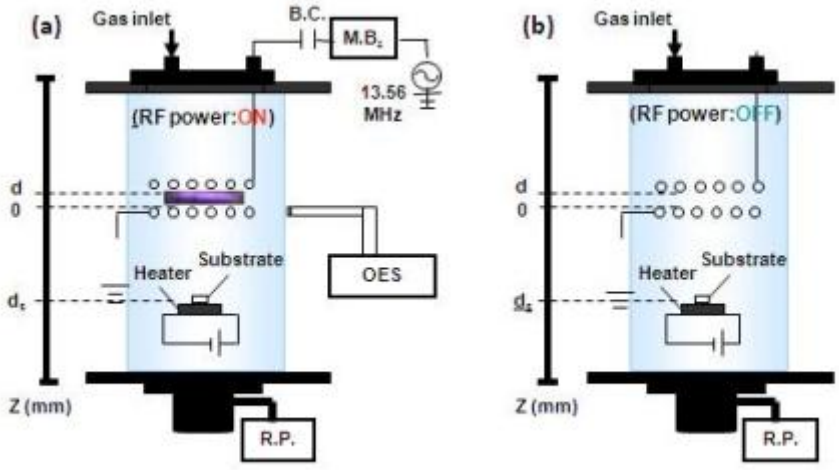

Fig. 2. Schematic diagram of experimental setups for (a) PCVD, and (b) TCVD.

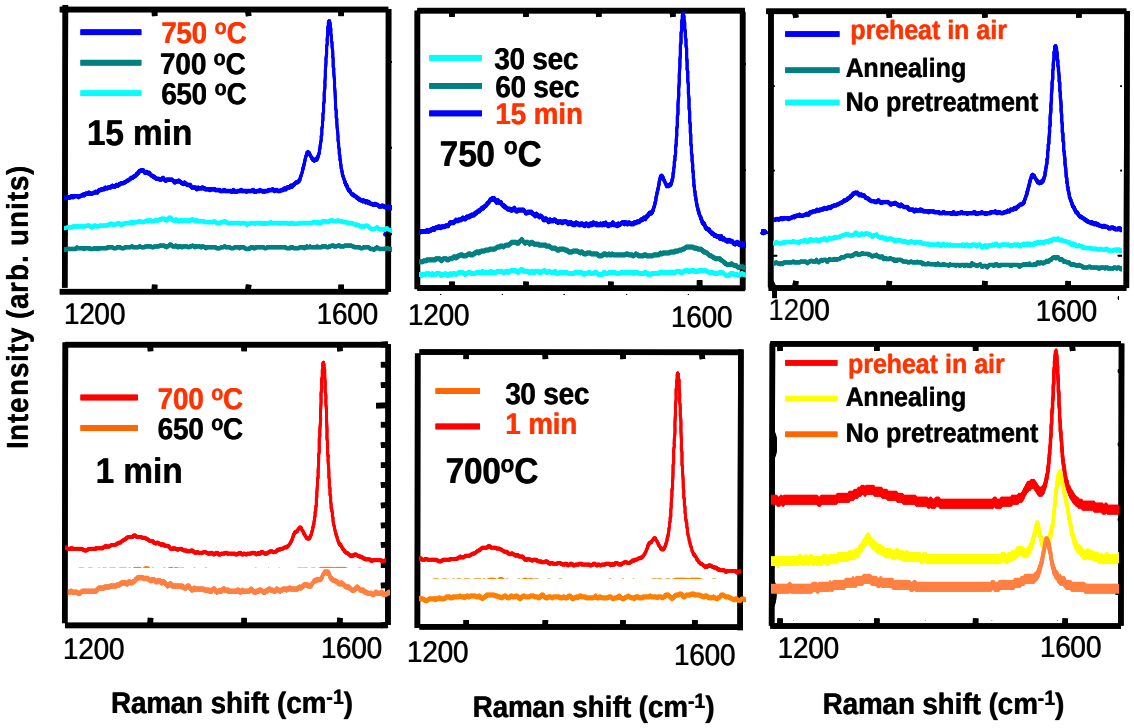

Fig. 3. Raman spectra of Au catalyzed SWNTs with (a-c) TCVD and (d-f) PCVD for different (a, d) growth time

cleaning of the Au catalyst, which achieves an effect similar to the pretreatment in air annealing. This indicates that the growth of SWNTs from the Au catalyst is strongly influenced by the surface condition of Au catalyst. Figure 4 gives a typical scanning electron microscopy (SEM, Hitachi S-4100) and a transmission electron microscopy (TEM, Hitachi HF-200) image of

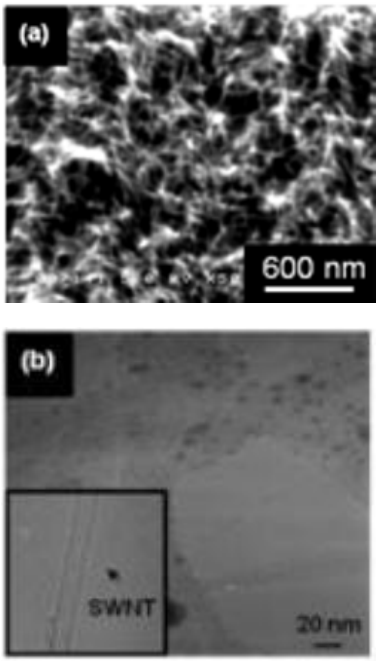

Fig. 4. Typical SEM (a) and TEM (b) images of Au catalyzed SWNTs by PCVD. Inset of (b) shows the high magnification image of individual SWNT.

SWNTs grown by Au-PCVD. Abundant SWNTs are found to be grown on a substrate (Figure 4(a)) with high yield (Figure 4(b)). Figures 5(a) and 5(b) show histograms of intensity ratio of G-peak to D-peak (I_G/I_D) estimated from Raman spectra as functions of RF power (P_{RF}) and electrode-substrate distance (d_{es}), where I_G/I_D gives a quantitative indication of the relative quality of SWNTs. When the radial breathing mode (RBM) in a lower wavenumber region (100 ~ 350 cm^{-1}) and G-band split (G^+ andG^-) are clearly observed, we judge that SWNTs are definitely grown. The Au catalyzed SWNTs growth with PCVD (Au-PCVD) (Fig. 5(a)) possesses a narrower process window due to the lower catalytic activity of the Au catalyst in comparison with Fe catalzed PCVD (Fe-PCVD) (Fig. 5(b)). The I_G/I_D does not differ between the Au and Fe catalysts under the best condition (P_{RF} = 50 W and d_{es} = 5 cm). All of the SWNTs growth processes with PCVD described hereafter are carried out under the optimum conditions for SWNT growth. PLE mapping [20] is used to assign (n,m) of SWNTs grown from the Au catalyst at different H_2 concentrations (Figs. 6(a-c)). Photoluminescence-excitation (PLE) measurements are performed utilizing a Nanolog (Horiba/Jobin yvon). A 450 W Xenon lamp is used to supply the excitation light in the 500-752 nm range in 4 nm steps. Photoluminescence (PL) spectra are recorded using a liquid nitrogen-cooled InGaAs array detector in the 900-1400 nm range. The slit width used for emission and excitation is 10 nm. The sample for PLE measurement is prepared by the following process. Several (5 ~ 10) as grown SWNTs samples made under the same growth condition are

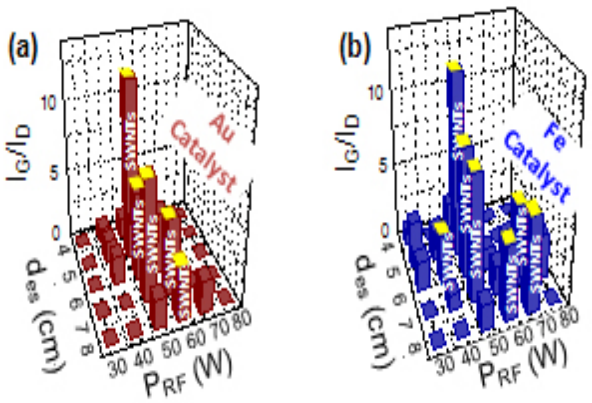

Fig. 5. (a) Histogram of I_G/I_D as functions of P_{RF} and d_{es} for SWNTs grown from (a) Au and (b) Fe catalysts with PCVD.

dispersed by 1 hour in ethanol of a bath type sonicator. After removing the substrate, the solution is settled down for a while until a precipitate of SWNTs appears on the bottom of the vial. Then ethanol solution is carefully removed and evaporated by a hot plate heating. The aqueous sodium dodecylbenzene sulfonate (SDBS) surfactant [2% by weight (2 wt %)] is added and treated in a needle-type sonicator for 4 h at a power level of 150 W. Immediately after sonication, samples are centrifuged at 54,000 g for 12 hours. The upper 75 to 80% of supernatant is then carefully decanted, leaving micelle-suspended nanotube solutions. In order to carry out a Raman scattering measurement for the exactly same sample measured by PL, a few drop of the solution used for PL measurement is dropped on a substrate. Raman scattering spectra are taken by micro-Raman scattering spectroscopy (Horiba/Jobin yvon) with 632.8 nm He-Ne and 778 nm semiconductor laser excitation. The total pressure is kept at 50 Pa by adjusting the pumping effeciency of rotary pump throughout this experiment. Lower H_2 concentrations (0 and 3-sccm) lead to growing larger diameter tubes and more widely (n,m)-distributed tubes with (6,5), (7,5), (7,6), (8,4), (8,6), and (8,7) (Figs. 6(a and b)). On the other hand, the 7-sccm H_2 concentration yields the narrowest (n,m) distribution with a dominant peak corresponding to the (6,5) tube. The UV-vis-NIR optical absorbance spectra of Au-PCVD SWNTs grown at the 7-sccm H_2 flow rate show one dominant peak in the first van Hove E_{11} range (900-1400 nm) corresponding to SWNTs with (6,5) chirality (Fig. 6(d)). Since clear metallic SWNTs peaks could not be observed in the UV-vis-NIR spectra (Fig. 6(d)), the concentration of metallic SWNTs can be lower than generally grown SWNTs. RBM in the Raman spectra measured with 632.8 nm and 778 nm lasers on the same SWNTs sample also confirms the growth of the (6,5) SWNTs (Fig. 6(e)). This is the first result realizing the narrow chirality distribution of SWNTs grown from a nonmagnetic catalyst. In order to elucidate the effects of Au and PCVD on the narrow chirality distribution,

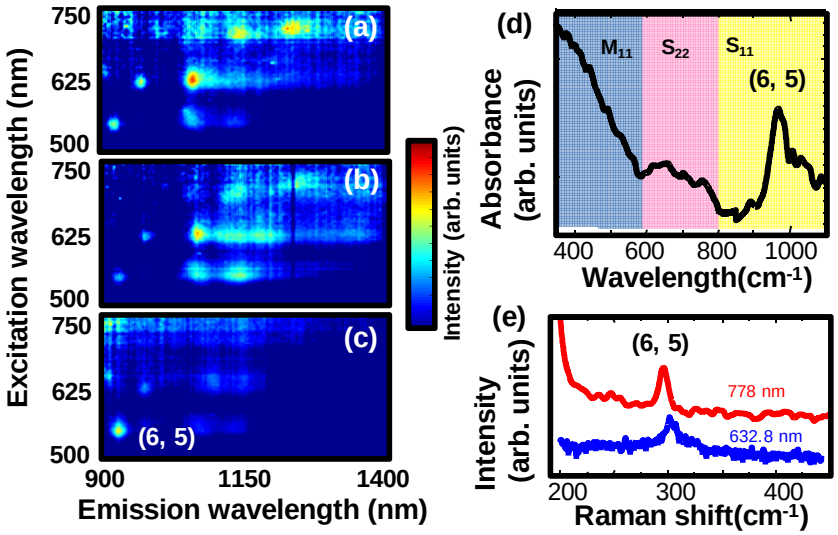

Fig. 6. (a-c) PLE maps of SWNTs from Au catalyst by PCVD at, 0-sccm, 3-sccm, and 7-sccm H_2 flow rates, respectively. (d) UV-vis-NIR spectrum of SDBS-dispersed SWNTs grown from Au catalyst at 7-sccm H_2 flow rate and (e) Raman spectra of SWNTs grown from Au catalyst at 7-sccm H_2 flow rate using the excitation laser wavelengths of 632.8 and 778 nm.

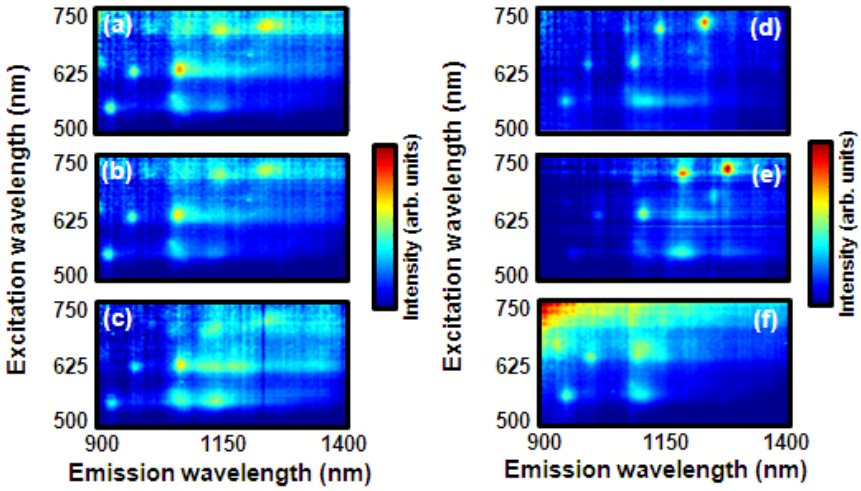

Fig. 7. PLE maps of (a-c) Fe-PCVD and (d-f) Au-TCVD SWNTs at different H_2 flow rates of; (a and d) 0 sccm, (b and e) 3 sccm, and (c and f) 7 sccm, respectively.

other combinations of catalyst types and CVD methods are taken up and systematically investigated. Based on the PLE analysis, SWNTs grown by the Fe catalyst with PCVD (Fe-PCVD) do not designate any clear dependence in the chirality distribution on the H_2 flow rate, which is fairly broader than that of Au-PCVD (Figs. 7 (a-c)). This indicates hydrogen-assisted Au catalyzation is one of the critical factors to realize the narrow chirality distribution, which is in good agreement with theoretical predictions. The first-principle calculation by Yazyev et al. [21] reveals that coinage metals such as Cu, Ag, and Au produce narrow chirality distributions. Ding et al. [22] report the SWNTs diameter is larger on the surface of Fe, Co, and Ni particles than Cu, Pd, and Au particles because of the different bond energies on the catalyst surface. Following these theoretical models, we can explain the effect of H_2-assisted Au catalyzation on the narrow chirality distirbution as follows, since the binding energy of hydrocarbons on the Au surface is much weaker than that on the Fe surface, it is difficult in the large-diameter case of Au catalyst to achieve the cap formation [22]. Additonal H_2 also enhances the etching of carbon precursor from the catalyst surface, which strongly suppresses the growth of large diameter SWNTs, and hence the chirality distribution grown from the Au catalyst can be narrower than that from the Fe catalyst. The stability of the cap structure migh be a possible reason why the (6,5) tube is dominant in this small diameter Au-PCVD SWNTs. The number of cap structures, which satisfy the isolated pentagon rule, is highly limited for small

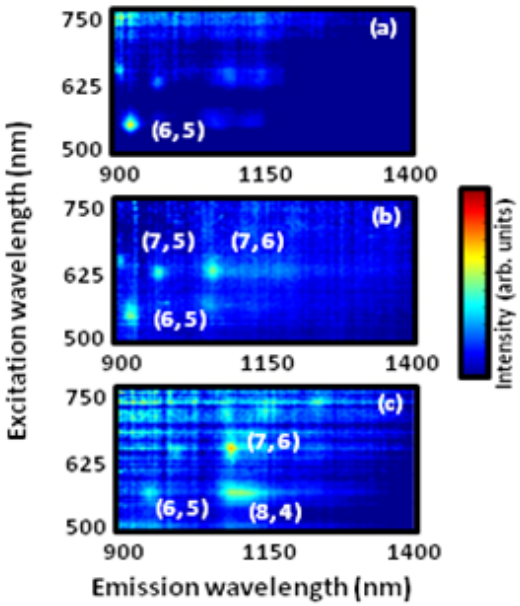

Fig. 8. PLE map of Au-PCVD SWNTs grown under different growth conditions. (a) P_{RF} = 50 W without pretreatment. (b) P_{RF} = 50 W with preheating in air. (c) P_{RF} = 60 W without pretreatment.

diameter SWNTs, and (6,5) is known to have one of the stable cap structures in this diameter range [13]. The comparison of Au-PCVD and Au-TCVD is also carried out. Although the chirality distribution becomes relatively narrow for the case of SWNTs grown even by Au-TCVD under appropriate H_2 concentrations, it is much broader than that of SWNTs grown by Au-PCVD (Figs. 7(d-f)). When we carefully compare the Au-PCVD and Au-TCVD processes, there are two significant differences in the SWNTs growth conditions. The first one is the growth temperature. The lower limit of growth temperature with Au-PCVD is 700 °C, which is lower than that of Au-TCVD (50 °C). The second one is the incubation time. The initial SWNTs growth is attained in 1 min after the growth substrate is exposed to the plasma in the case of Au-PCVD, whereas 15 min is required for the growth of SWNTs with Au-TCVD. These results suggest that the low temperature and short time growth with Au-PCVD can avoid an aggregation of catalyst particles during the SWNTs growth, which suppresses the growth of large diameter SWNTs, resulting in the narrow chiratliy distribution. In order to support the validity of the explanation for narrow-chirality distributed growth over Au under PCVD with appropriate hydrogen concentration, the PLE measurement is carried out under different growth conditions. Fig. 6(c) is re-used to produce Fig. 8(a). The growth condition of this sample is RF input power (P_{RF}) of 50 W without any pretreatment. When pre-heating in air is performed as a pretreatment which is necessary in Au-TCVD, the selectivity of (6,5) SWNTs decreases and the growth of other chiralities of (7,5) and (7,6) are enhanced (Fig. 8(b)). This can be due to the increment of the catalyst size during the pretreatment. When we increase the P_{RF} up to 60 W without any pretreatment, the chirality distribution becomes broad and larger SWNTs tend to be grown as shown in Fig. 8(c). Since the amount of carbon reactants can be increased with an increase in the P_{RF}, larger catalyst particles might be more activated, resulting in the broadening of the chirality distribution. Small catalyst particles might be deactivated by an over supplying of carbon precursors. These indicate that the growth window of the narrow-chirality distributed SWNTs in Au-PCVD is very narrow, and precise adjustment of growth condition is required. The electrical features are also investigated for the SWNTs grown by Au-PCVD, Fe-PCVD, Au-TCVD, and Fe catalyzed TCVD (Fe-TCVD). As-synthesized SWNTs are dispersed in 1 ml of dimethylformamide (DMF) under ultrasonication for 8 hours, followed by spin coating between source and drain electrodes of a field effect transistor (FET). In order to compare the bulk SWNTs features, the transport measurements are carried out under the thin film FET configuration including multi-conducting channels. We investigate more than 30 such FET devices, and a typical source-drain current (I_{ds}) vs gate bias voltage (V_{gs}) curve is shown in Fig. 9(a). The percentage of semiconducting devices for each case is calculated in Fig. 9(b) using the I_{ds} vs V_{gs} curves by dividing the number of devices which have the on-off current ratio (I_{on}/I_{off}) greater than 20 by the total number of the conducting devices.

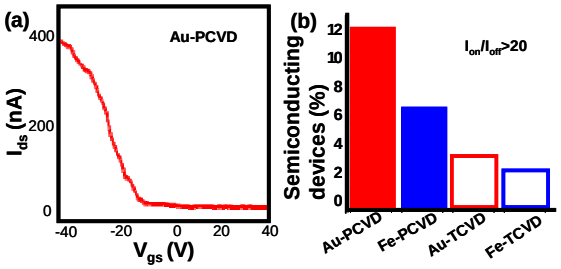

Fig. 9. (a) Typical I_{ds}-V_{gs} curve of the thin film FET for Au-PCVD SWNTs. (b) Percentage histogram of semiconducting devices depending on the combinations of catalyst types and CVD methods.

In the case of TCVD, the percentage of semi-conducting devices (I_{on}/I_{off} > 20) is almost the same for both the catalysts (Au and Fe). When it comes to the PCVD case, the Au-PCVD SWNTs display the highest concentration of the semico-nducting device, which can be attributable to the high percentage of semiconducting SWNTs [23] prepared by PCVD [24] in addition to the narrow chirality distribution realized by the Au catalyst. In order to measure the magnetic properties of the Au synthesized SWNTs, firstly the SWNTs are dispersed in the ethanol and then dropped on the quartz substrate for the measurement. The sam-

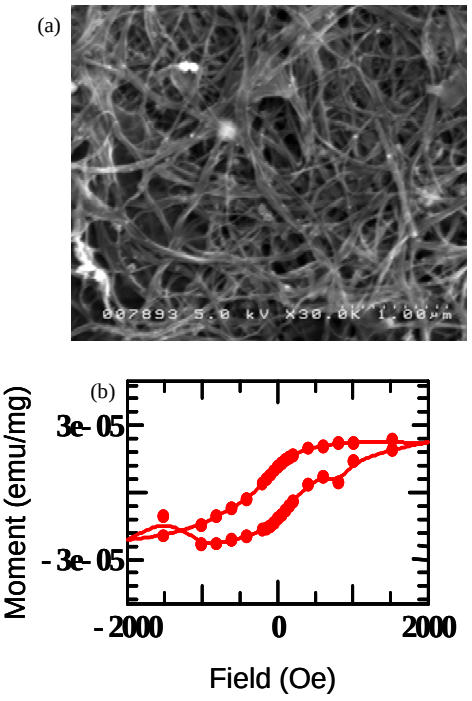

Fig. 10. (a) SEM image and (b) magnetization per mg vs applied magnetic field for the Au-PCVD SWNTs.

ple is placed between two magnets and by applying the magnetic field the induced magnetic field can be estimated. Figs. 10(a) and (b) show the SEM image and induced magnetization vs, applied magnetic filed graph for the Au synthesized SWNTs by PCVD method, respectively. Fig. 10(a) confirms the high purity of the non-purified SWNTs grown by PCVD method over the Au catalyst. Fig. 10 (b) suggests that the SWNTs grown from the nonmagnetic catalysts show the ferromagnetic features. From the magnetization vs. magnetic field graph it turns out that saturation magnetization (M_s) is of the order of 10^{-5}, which show the weak ferromagnetic features but in order to study the origin of the ferromagnetism in the Au synthesized SWNTs, the magnetic properties of the Au catalyst is also checked. SQUID measurement of the Au catalyst confirms the diamagnetic behavior of the Au catalyst particles. Apart from magnetic catalyst impurities, intrinsic defects are also known to be responsible for appearance of magnetism in carbon materials.

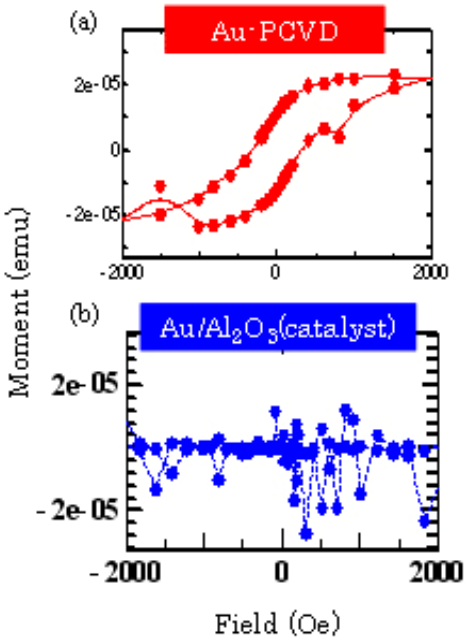

Fig. 11. Magnetization of the sample vs applied magnetic field for (a) the AuPCVD SWNTs and (b) Au catalyst.

Fig. 11(a) and (b) show the ferromagnetic and diamagnetic features of the Au-SWNTs and Au particles for the total sample measured, respectively. These results suggest that the origin of the ferromagnetic features of the Au-SWNTs might be due to the SWNTs itself. Hence nonmagnetic synthesized SWNTs might be useful for further studies on the intrinsic magnetic properties of the SWNTs and also the chirality dependence of the SWNTs magnetic properties. On the other hand, magnetic CNTs can be successfully used both as cantilever tips in magnetic force microscopy (MFM) and as a nanocontainer for new therapies in medicine. Since iron and other magnetic nanoparticles might be toxic, using the nonmagnetic catalyst of the Au for the SWNTs growth can be useful for medical applications of the SWNTs.

4. Conclusion

In conclusion, we have for the first time demonstrated the narrow-chirality distributed growth of SWNTs from the nonmagnetic catalyst. The Au catalzed PCVD growth under the appropriate hydrogen concentration is figured to be the critical factor in achieving the narrow chirality distribution. This narrow-chirality distributed SWNTs selectively grown from the nonmagnetic catalyst could be attractive to both fundamental studies of intrinsic magnetic properties of SWNTs and industrial applications to nanoelectronics.

References

[1] S. Ijima, Nature **354**, 56 (1991).
[2] R. Saito, G. Dresslhaus, M. S. Dresselhaus, *physical properties of carbon nanotubes*, Imperical college Press, London, (1998).
[3] H. T. Soh, C. F. Quate, A. F. Morpurgo, C. M. Marcus, J. Kong, H. Dai, Appl. Phys. Lett. **75**, 627 (1999).
[4] W. B. Choi, D. S. Chung, J. H. Kang, H. Y. Kim, Y. W. Jin, I. T. Han, Y. H. Lee, J. E. Jung, N. S. Lee, G. S. Choi, J. M. Kim, Appl. Phy. Lett. **75**, 3129 (1999).
[5] H. M. Cheng, Q. H. Yang, C. Liu, Carbon **39**, 78, 1447, (2001).
[6] A. B. Mendez, J. C. Delgado, A. M. Gomez, M. R. Herrera, A. G. Rodriguez, H. Navarro, M. A. Vidal, H. Terrones, and M. Terrones, Chem. Phys. Lett. **45**, 55 (2008).
[7] X. Li, X. Tu, S. Zaric, K. Welsher, W. S. Seo, W. Zhao, and H. Dai, J. Am. Chem. Soc. **129**, 15770 (2007).
[8] Y. Li, D. Mann, M. Rolandi, W. Kim, A. Ural, S. Hung, A. Javey, J. Cao, D. Wang, E. Yenilmez, Q. Wang, J. F. Gibbons, Y. Nishi, and H. Dai, Nano Lett. **4**, 317 (2004).
[9] L. Ding, A. Tselev, J. Wang, D. Yuan, H. Chu, T. P. McNicholas, Y. Li, J. Liu, Nano Lett. **9**, 800 (2009).
[10] D. Takagi, Y. Homma, H. Hibino, S. Suzuki, Y. Kobayashi, Nano Lett. **6**, 2642 (2006).
[11] M. Ritschel, A. Lenonhardt, D. Elefant, S. Oswald, B. Buchner, J. Phys. Chem. **111**, 8414 (2007).
[12] D. Yuan, L. Ding, H. Chu, Y. Feng, T. P. Mcnicholas, J. Liu, Nano Lett. **8**, 2082 (2008).
[13] D. Takagi, Y. Kobayashi, H. Hibino, S. Suzuki, Y. Homma, Nano Lett. **8**, 3 (2008).
[14] T. Kato, G.-H. Jeong, T. Hirata, R. Hatakeyama, K. Tohji, and K. Motomiya, Chem. Phys. Lett. **381**, 422 (2003).
[15] T. Kato, and R. Hatakeyama, Appl. Phys. Lett. **92**, 031502 (2008).
[16] T. Kato, R. Hatakeyama, K. Tohji, Nanotechnol. **17**, 2223 (2006).
[17] E. J. Bae, Y.-S. Min, D. Kang, J.-H. Ko, W. Park, Chem. Mater. **17**, 5141 (2005).
[18] L. Qu, F. Du, and L. Dai, Nano Lett. **8**, 2682 (2008).
[19] M. Haruta., Catal. Today **36**, 153 (1997).
[20] O. V. Yazyev, A. Pasquarello, *Phys. Rev. Lett*. **100**, 156102 (2008).
[21] A. F. Ding, P. Larsson, J. A. Larson, R. Ahuja, H. Duan, A. Rosen, K. Bolton, *Nano Lett.* **8**, 463 (2008).
[22] S. M. Bachilo, L. Balzano, J. E. Herrera, F. Pompeo, D. E. Resasco, R. B. Weisman, J. Am. Chem. Soc. **125**, 11186 (2003).
[23] B. Liu, W. Ren, C. Liu, C. H. Sun, L. Gao, S. Li, C. Jiang, H. M. Cheng, *ACS Nano* **3**, 3421 (2009).
[24] Y. Li, D. Mann, M. Rolandi, W. Kim, A. Ural, S. Hung, A. Javey, J. Cao, D. Wang, E. Yenilmez, Q. Wang, J. F. Gibbons, Y. Nishi, H. Dai, *Nano Lett.* **4**, 317 (2004).